INFECTION AND IMMUNITY, Oct. 2001, p. 6391–6400 Vol. 69, No. 10
0019-9567/01/$04.00+0 DOI: 10.1128/IAI.69.10.6391–6400.2001

Macrophage Nitric Oxide Synthase Associates with Cortical Actin but Is Not Recruited to Phagosomes

J. L. WEBB, M. W. HARVEY, DAVID W. HOLDEN, AND T. J. EVANS*

Department of Infectious Diseases, Imperial College School of Medicine, Hammersmith Hospital, London W12 0NN, United Kingdom

Received 24 January 2001/Returned for modification 24 April 2001/Accepted 11 July 2001

Nitric oxide (NO) produced from inducible NO synthase (iNOS) is an important component of host defense against intracellular pathogens. To understand how phagocytes deliver NO to ingested microorganisms while avoiding cytotoxicity, we set out to study the subcellular localization of iNOS within macrophages following phagocytosis. Confocal microscopy of immunostained cells showed that iNOS was located not only diffusely within cytoplasm but also in vesicles, as well as immediately adjacent to the peripheral cell membrane. This peripheral iNOS colocalized with the cortical actin cytoskeleton and was removed by the actin-depolymerizing drug cytochalasin B. Biochemical fractionation of RAW 264 macrophages showed that 32.75% (±5.11%; $n = 3$) of iNOS was present in a particulate fraction, which cosedimented with low-density cellular vesicles. Following phagocytosis of latex beads, zymosan, immunoglobulin G-coated beads, or complement-coated zymosan, submembranous cortical iNOS was not recruited to phagosomes, nor was there any relocalization of intracellular iNOS. Similarly, following phagocytosis of *Salmonella enterica* serovar Typhimurium there was no recruitment of iNOS to the *Salmonella* vacuole at any stage after internalization. NO mediated significant killing of intracellular *S. enterica* serovar Typhimurium in RAW macrophages treated with lipopolysaccharide and gamma interferon; this was evident 4 h after infection. Although not recruited to phagosomes, iNOS association with the submembranous cortical actin cytoskeleton is ideally suited to deliver NO to microbes in contact with the cell surface and may contribute to early killing of ingested *Salmonella*.

Nitric oxide (NO) plays important roles in many different aspects of mammalian biology (25). In phagocytes, NO is produced in large quantities by the action of the enzyme inducible NO synthase (iNOS), also known as type II NOS (20, 33). This isoform is produced following stimulation of cells with agents such as inflammatory cytokines and lipopolysaccharide (LPS). Studies using NOS inhibitors and mice with targeted disruption of the iNOS gene have demonstrated an important role of NO release from this enzyme in host defense against a number of intracellular pathogens, including *Mycobacterium tuberculosis*, *Leishmania major*, *Listeria monocytogenes*, and *Salmonella enterica* serovar Typhimurium (26, 32).

NO is a highly reactive free radical with antimicrobial activity on its own, but it also can form a number of oxidation products such as NO_2, NO_2^-, N_2O_3, and *S*-nitrosothiols. In addition, it reacts with superoxide to yield the extremely reactive and microbicidal peroxynitrite anion, $ONOO^-$ (2, 41). Collectively, these reactive nitrogen intermediates have a spectrum of antimicrobial activity mediated by their ability to react with key protein and lipid molecules in microbes (18, 29). These cytotoxic effects are not restricted to microbes, as reactive nitrogen intermediates can act on host cells to produce cell necrosis or apoptosis, thus potentially exacerbating tissue injury where produced (5, 19).

This balance between microbicidal activity and potential cytotoxicity applies to many of the antimicrobial products produced by phagocytes, such as lysosomal enzyme products and superoxide. How do these cells avoid the damaging effects of these chemicals, while still efficiently killing invading pathogens? One mechanism is by compartmentalizing these toxic compounds within the cell so that they are released in close proximity to the pathogen, for example, by fusion of lysosomes with phagosomes or targeting of the superoxide-generating cytochrome *b* to neutrophil-specific granules (4, 8, 23). Pathogens also have strategies to avoid these compartmentalized killing compounds. For example, *S. enterica* serovar Typhimurium disrupts intracellular trafficking and avoids fusion with lysosomal contents (7). It also prevents movement of active NADPH oxidase to the *Salmonella* vacuole (38). This effect on the movement of NADPH oxidase is mediated by a type III secretion system encoded within *Salmonella* pathogenicity island 2 (SPI-2) (38). However, NO still has an important antimicrobial effect against serovar Typhimurium, mainly by exerting a relatively delayed bacteriostatic effect within macrophages (37).

In neutrophils, we have shown that iNOS is localized to primary granules, where it is able to mediate nitration of ingested bacteria, most likely through the generation of peroxynitrite (13). In macrophages, although the enzyme is frequently described as cytoplasmic, some reports have shown that a proportion of the enzyme is localized to a particulate fraction within the cell (17, 30). One study has addressed the subcellular localization of iNOS within primary macrophages, using immunoelectron microscopy (39). This found that a proportion of iNOS was present in a population of vesicles, most notably in the *trans*-Golgi network. The authors reported that iNOS was not associated with phagosomes containing *Mycobacterium avium* or *Leishmania mexicana,* although a preliminary association of iNOS vesicles with phagosomes containing

* Corresponding author. Mailing address: Department of Infectious Diseases, Imperial College School of Medicine, Hammersmith Hospital, Du Cane Rd., London W12 0NN, United Kingdom. Phone: 44 20 8383 8576. Fax: 44 20 8383 3394. E-mail: tom.evans@ic.ac.uk.

immunoglobulin G (IgG)-coated beads was mentioned. However, no images of the distribution of iNOS following phagocytosis were presented.

Once iNOS has been induced within the macrophage, there appear to be few further controls over its activity (27), although the availability of tetrahydrobiopterin and L-arginine may be important (31, 34). Given the high reactivity of NO, we postulated that one way in which the cell could control the delivery of NO to its targets would be by subcellular compartmentalization, specifically to phagosomes. Using high-resolution laser confocal immunofluorescence microscopy and biochemical techniques, we found in both primary murine macrophages and the macrophage cell line RAW264 stimulated with LPS and gamma interferon (IFN-γ) that a proportion of iNOS was associated with the cortical submembranous actin cytoskeleton, as well as in intracytoplasmic vesicles and in free cytoplasm. Following phagocytosis of a variety of particles or the pathogen *S. enterica* serovar Typhimurium, membrane-associated iNOS did not relocalize around phagosomes, nor was there recruitment of cytoplasmic iNOS to phagosomes. However, NO mediated a significant killing effect against serovar Typhimurium within 4 h of infection in LPS- and IFN-γ-treated cells that may be mediated by membrane-associated iNOS.

MATERIALS AND METHODS

Reagents and antibodies. Rabbit polyclonal (N32030) and murine monoclonal (N39120) antibodies to iNOS were from Transduction Laboratories, Lexington, Ky., as was mouse monoclonal antibody to GM130. Goat polyclonal anti-LAMP1 was from Santa Cruz Biotechnology. Secondary antibodies conjugated to Alexafluors were from Molecular Probes (Eugene, Oreg.). Biotinylated secondary antibodies to mouse, rabbit, or goat immunoglobulin were from Jackson ImmunoResearch Laboratories, West Grove, Pa., or Vector Laboratories, Peterborough, United Kingdom. Fluorescein isothiocyanate or Texas red avidin was bought from Vector Laboratories. Latex beads and zymosan particles were from Sigma-Aldrich, Poole, United Kingdom. Wild-type *Salmonella enterica* serovar Typhimurium 12023, its corresponding SPI-2 mutant, and the green fluorescence protein-labeled wild-type strain were as previously described (3).

Cell culture. To obtain peritoneal macrophages, CD1 mice were primed with thioglycolate broth or BioGel P100 beads (Bio-Rad, Hercules, Calif.). Three days later, peritoneal fluid was collected and cells were washed in Hanks balanced salt solution (Life Technologies Ltd., Paisley, United Kingdom) and plated out for 2 h at 37°C. Adherent macrophages were then washed free of other cells. Cells were seeded onto glass coverslips (Merck Ltd., Poole, United Kingdom) in 24-well dishes (Corning Costar, High Wycombe, United Kingdom) at 10^6 cells ml^{-1}. Both RAW 264 cells and primary macrophages were cultured in Dulbecco's modified Eagle's medium (Life Technologies Ltd.) with 10% heat-inactivated fetal calf serum (Labtech International, Ringmer, United Kingdom) and 1 mM glutamine (Life Technologies Ltd.). Where indicated, cells were stimulated for 18 h with 10 ng of IFN-γ (Peprotech EC Ltd., London, United Kingdom) ml^{-1} and 2 μg of LPS from *Escherichia coli* serotype 0111:B4 (Sigma-Aldrich) ml^{-1}. If used, cytochalasin B (Sigma-Aldrich) was added to cells at 10 μM for 30 min. Particles were centrifuged onto the macrophages at 450 × *g* for 2 min, normally at a ratio of 10 to 1. Zymosan was prepared by being boiled in phosphate-buffered saline (PBS; 0.01 M sodium phosphate buffer [pH 7.3], 0.15 M NaCl) for 30 min. Bacteria were used at stationary phase or logarithmic phase, opsonized in 10% mouse serum (Serotec Ltd., Oxford, United Kingdom) for 15 min at 37°C, and then washed three times with PBS before being added to macrophages.

Immunostaining. iNOS was detected by immunocytochemistry using either a murine monoclonal iNOS antibody or a rabbit polyclonal anti-iNOS (both from Transduction Laboratories). The monoclonal antibody recognizes a single 135-kDa protein, the expected weight of iNOS, in cytokine-treated human and murine cells (28, 40). After incubation, cells were washed gently three times with PBS and left to dry. Cells were fixed in 1% paraformaldehyde for 30 min, washed in PBS, and then blocked in 0.2 M glycine in PBS for 15 min. Cells were washed three times in PBS and then permeabilized in 0.1% Triton X-100 in PBS for 15 min. After further washes in PBS, cells were blocked in 10% serum (Serotec Ltd.), using animal serum corresponding to the host in which the secondary antibody was derived. After at least 30 min of incubation, the block was removed and primary antibody to iNOS was added. Cells were incubated for 18 h at 4°C. After three 5-min washes in PBS, secondary antibody to mouse or rabbit was added either using Alexafluor conjugates (Molecular Probes Europe BV, Leiden, The Netherlands) or adding the appropriate biotinylated secondary antibody (Vector Laboratories or Jackson ImmunoResearch Laboratories) and then adding fluorescein isothiocyanate or Texas red-conjugated avidin (Vector Laboratories). Tetramethyl rhodamine isocyanate-phalloidin (Sigma-Aldrich) was used to detect filamentous actin. After washing, DAPI (4′,6′-diamidino-2-phenylindole) (Sigma-Aldrich) was added to stain nuclei. Cells were mounted in Vectashield (Vector Laboratories). Immunofluorescent images were acquired by confocal microscopy, using a Zeiss Axiovert microscope and the Bio-Rad MRC 1024 Confocal system, running with LaserSharp software.

Sodium dodecyl sulfate-polyacrylamide gel electrophoresis and immunoblotting. To extract sufficient protein for Western analysis, 12 175-cm^2 flasks of RAW cells were used for each fractionation, using a published method (35). Briefly, cells were stimulated with 10 ng (200 U) of IFN-γ per ml and 2 μg of LPS ml^{-1} for 18 h and then scraped into 1 ml of lysis buffer (0.25 M sucrose, 3 mM imidazole, 0.5 mM EDTA [pH 7.3]) containing 1 μg each of leupeptin, aprotonin, chymotrypsin inhibitor, and antipain ml^{-1}. Cells were centrifuged at 750 × *g* for 7 min, and the cell pellet was resuspended in 100 μl of lysis buffer. This suspension was passed through a 21-gauge needle until cell breakage occurred, and then it was centrifuged at 750 × *g* for 7 min to remove nuclei. The supernatant was then centrifuged at 100,000 × *g* for 2 h to separate soluble and particulate fractions. The pellet, containing particulate material, was resuspended in 1 ml of lysis buffer, vortexed gently, and left on ice for 30 min. It was then layered onto 9 ml of 17% Percoll, which was above a cushion of 2 ml of 64% sucrose, both made up in lysis buffer. Tubes were centrifuged at 56,000 × *g* for 1 h (without the brake) and 1-ml fractions were recovered by puncturing the tube. Fractions were run on an 8% acrylamide sodium dodecyl sulfate-polyacrylamide gel electrophoresis gel and blotted onto a polyvinylidene difluoride membrane (Amersham Pharmacia Biotech UK, Little Chalfont, United Kingdom). iNOS was detected with a monoclonal iNOS antibody (Transduction Laboratories) and biotinylated secondary anti-mouse antibody (Vector Laboratories and Jackson ImmunoResearch Laboratories), horseradish peroxidase-streptavidin reagent (Serotec Ltd.), and ECL plus detection (Amersham Pharmacia Biotech UK). To identify cell surface proteins, cells were treated with biotinylation reagent EZ-Link Sulfo-NHS-LC-Biotin (Pierce Chemical Company, Rockford, Ill.) before being scraped into lysis buffer. To identify fractions containing transferrin (early endosomes), 20 nM biotin-transferrin (Molecular Probes) was added to unstimulated RAW cells and incubated for 20 min at 37°C before being washed with PBS, and cells were scraped from the flask in 1 ml of lysis buffer.

Quantification of iNOS protein within particulate and soluble fractions was determined by densitometric analysis of Western blots in a linear range of exposure. Results are expressed as a percentage of the total iNOS present within the cell lysate.

iNOS activity assay. Fractions and totals were assayed for iNOS activity by following the conversion of [^{3}H]arginine to citrulline (NOS*detect* Assay Kit; Stratagene, Amsterdam, The Netherlands). To duplicate reaction mixtures, we added 2 mM L-NIL hydrochloride (Calbiochem-Novabiochem [UK] Ltd., Nottingham, United Kingdom) to identify iNOS-dependent conversion to L-citrulline. Reactions were carried out according to the kit instructions, and L-citrulline was recovered by adding the reaction mixture to columns containing DOWEX 50WX8-400 ion-exchange resin (Sigma-Aldrich) and washing it three times with water to elute citrulline. The quantity of isotope was measured by liquid scintillation counting.

β-Glucuronidase assay. To identify fractions containing lysosomes, we assayed the presence of β-glucuronidase activity by using a diagnostic kit (Sigma-Aldrich). Briefly, 20 μl of each fraction was mixed with 20 μl of phenolphthalein glucuronic acid solution and 60 μl of acetate buffer solution and incubated at 56°C for 1 h. Five hundred microliters of 2-amino-2-methyl-1-propanol buffer was added, and absorbance was read at 550 nm.

Assay of intracellular *Salmonella* viability. Monolayers of RAW macrophages in 24-well plates (10^6 cells per well) treated as described above were infected with opsonized *Salmonella enterica* serovar Typhimurium 12023 in the stationary phase of growth at a multiplicity of infection of 10. To ensure a synchronous infection, after the addition of bacteria plates were centrifuged at 200 × *g* for 4 min and then incubated at 37°C for 30 min. Gentamicin (12 μg ml^{-1}) was then added to kill extracellular bacteria, and incubation was continued as required. Viable intracellular bacteria were assayed by washing the well twice with PBS,

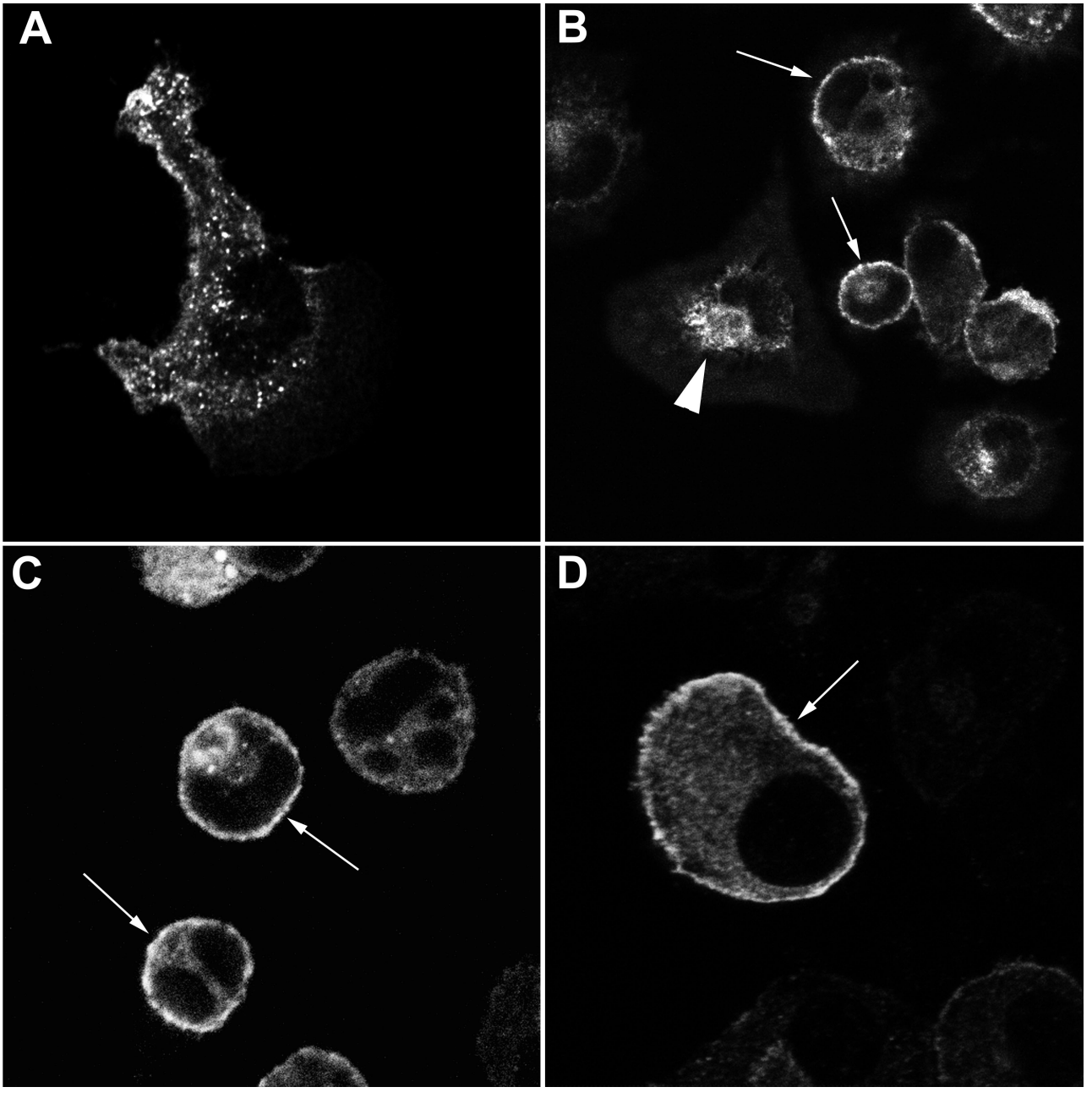

FIG. 1. Localization of iNOS within macrophages. Primary mouse peritoneal macrophages (A to C) or RAW 264 cells (D) were stimulated with IFN-γ alone (A) or with IFN-γ and LPS (B to D) and immunostained for iNOS, using the mouse monoclonal antibody. All images were obtained using laser confocal microscopy. Magnification, ×2,000 (A), ×600 (B to C), or ×6,000 (D). Arrows indicate peripheral plasma membrane staining of iNOS. The solid arrowhead in panel B indicates iNOS staining in the perinuclear area.

lysing the cells in 100 μl of 1% Triton X-100 for 10 min at room temperature, and plating serial dilutions onto prewarmed LB agar plates. After overnight culture at 37°C, CFU were enumerated. Each experimental point was determined in triplicate.

Statistical analysis. Results are given as the means plus or minus standard deviations. To calculate the percentage of cells expressing iNOS in the plasma membrane, a total of >50 iNOS-positive cells were scored in three to four separate experiments.

RESULTS

Immunofluorescent microscopic localization of iNOS within mouse macrophages. We used a mouse monoclonal anti-iNOS and a polyclonal rabbit anti-iNOS. The pattern of staining was identical with both antibodies used; isotype-matched control sera gave no immunostaining using both anti-mouse and anti-rabbit secondary reagents. Unstimulated cells showed only 0 to 1% iNOS-positive cells.

We first analyzed the pattern of iNOS staining in primary mouse peritoneal macrophages stimulated with IFN-γ or IFN-γ and LPS (Fig. 1A to C). Three main sites of staining could be visualized. First, virtually all cells showed a degree of diffuse intracytoplasmic staining, although this differed in intensity from cell to cell. Secondly, we found staining in discrete

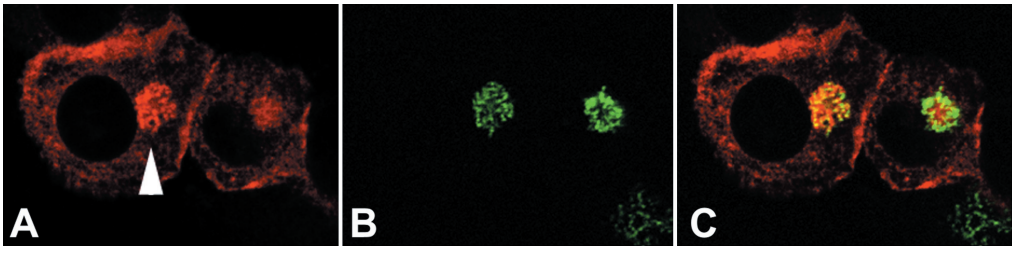

FIG. 2. iNOS can be found in the Golgi apparatus. RAW 264 cells were stimulated with LPS and IFN-γ and dually stained for iNOS using a rabbit polyclonal antibody, with red staining (A), and the intrinsic Golgi protein GM130, with green staining (B). (C) Merged images of panels A and B, with areas of colocalization in yellow. Magnification, ×1,000 for all panels.

intracellular punctate structures, consistent with a vacuolar localization of iNOS. These were either distributed fairly evenly within the cytoplasm (Fig. 1A) or in 5 to 10% of cells aggregated in the perinuclear area (Fig. 1B). The third site of staining was at the periphery of the cell, apparently in the region of the plasma membrane (Fig. 1B and C). Fifty-seven percent (±8.92%; $n = 4$) of cells showed some iNOS staining localized to this site. As the limit of resolution of confocal microscopy is about 0.5 μm, this immunostaining may be either in association with the membrane or immediately below it in the submembranous area. To avoid confusion, we term this peripheral staining cortical iNOS localization. The relative amount of iNOS in this cortical location, compared to an intracytoplasmic site, varied among different macrophage preparations. However, the cortical iNOS shown in Fig. 1B and C is representative of all the preparations. Quantification of the proportion of iNOS at this location is considered further below and in Discussion. We noted that the majority of cells with cortical iNOS had a rounded shape, while those that had extended one or more pseudopodia tended not to show peripheral iNOS staining (Fig. 1A and B).

We also examined the distribution of iNOS within IFN-γ- and LPS-treated RAW 264 cells, a mouse macrophage cell line. A similar pattern of distribution of staining was seen, with 43.3% (±8.79%; $n = 3$) of cells showing some cortical iNOS staining (Fig. 1D). In addition, in about 5 to 10% of cells we also observed the perinuclear staining seen in the primary macrophages. To determine whether iNOS in the perinuclear area was localized within the Golgi apparatus, we stained IFN-γ- and LPS-treated RAW cells for both iNOS and the intrinsic Golgi membrane protein GM130. In cells showing perinuclear iNOS (Fig. 2A), the pattern of GM130 staining (Fig. 2B) overlapped considerably with perinuclear iNOS staining (Fig. 2C). Not all the iNOS-positive vesicles in this area, however, colocalized with GM130, as the merged image of Fig. 2C shows some vesicles in the Golgi region that stain only with iNOS and thus are green in the merged image. However, in all instances where there was perinuclear iNOS staining we saw overlapping of most of the iNOS staining with that for GM130. These data suggest that some of the perinuclear iNOS staining observed is in the Golgi apparatus, although at least a proportion is in a vesicle population that does not contain GM130.

iNOS associates with actin at the cell periphery. We examined whether there was an association between iNOS and the cortical actin cytoskeleton that might account for its localization at the cell periphery. Using fluorescent phalloidin to visualize polymerized actin, we found that iNOS and polymerized actin colocalize at the cell periphery (Fig. 3A to C). When the cortical cytoskeleton was disrupted with cytochalasin B, cortical iNOS was completely disrupted, with iNOS distributed entirely within the cytoplasm (Fig. 3D to F). It is important to stress that following cytochalasin treatment, we were unable to detect any cell that showed cortical iNOS staining. These data suggest strongly that the peripheral iNOS is associated with the cortical actin cytoskeleton. To determine if any iNOS was exposed on the surface of cells, we immunostained macrophages for iNOS with no prior permeabilization step. Under these conditions, we observed no iNOS staining (data not shown). Taken together, these data suggest that iNOS associates with the cortical actin cytoskeleton at the cytoplasmic face of the plasma membrane.

Biochemical fractionation of iNOS within RAW 264 cells. In order to explore the subcellular distribution of iNOS further, we fractionated RAW 264 cells using biochemical techniques. We chose these cells for further study, as it was difficult to obtain enough material from primary peritoneal macrophages without sacrificing large numbers of animals. Particulate and soluble fractions were analyzed for the presence of iNOS by Western blotting. We found that 32.75% (±5.11%; $n = 3$) of total cellular iNOS was recovered in the particulate fraction as assayed by densitometry of immunoblots, in good agreement with other studies (30, 39). The activity of this particulate material was also measured and found to be 16.47% (±0.15%; $n = 3$) of total cellular iNOS activity. The smaller amount of iNOS activity in the particulate material, compared to the amount of iNOS protein, may reflect poor access of substrates and cofactors to the particulate enzyme or some denaturation on centrifugation, or it may truly reflect a difference in specific activity of iNOS in cytosolic and particulate locations.

We resuspended the particulate material and fractionated it by Percoll density centrifugation, using a protocol that separated plasma membrane and early endosomes from late endosomal and lysosomal vesicles (35). Western blotting of fractions from this gradient showed that most of the iNOS protein was found in the lightest fractions (Fig. 4A, lanes 1 to 3), although a small amount could be detected in the remaining denser fractions (Fig. 4A, lanes 4 to 11). To detect iNOS in these denser fractions required a film exposure that overexposes the iNOS signal in lanes 1 to 4, thus underestimating the percentage of iNOS in these fractions. Using shorter exposures, densitometry showed that 95% of particulate iNOS sedi-

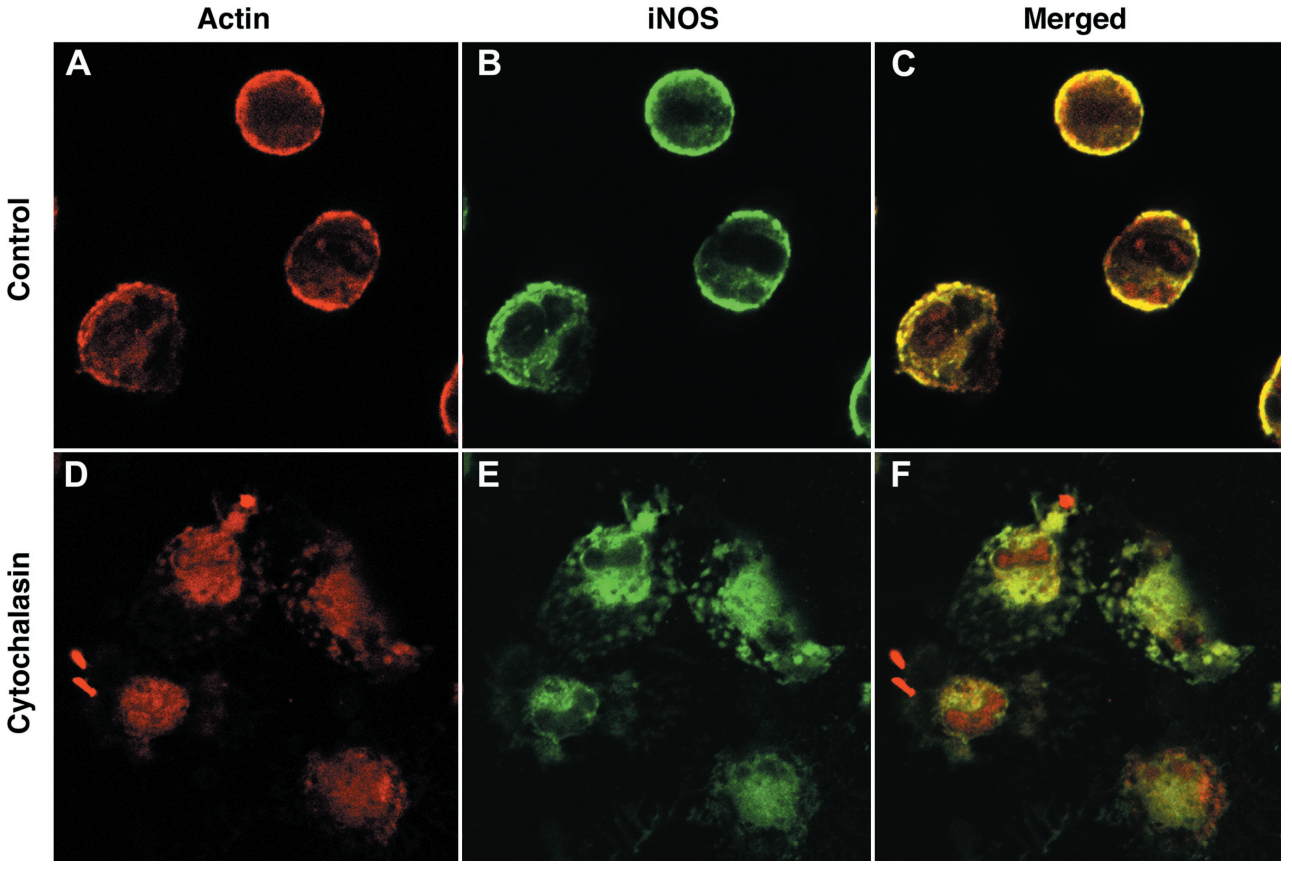

FIG. 3. iNOS associates with the cortical actin cytoskeleton. Primary peritoneal macrophages were stimulated with LPS and IFN-γ and immunostained for iNOS with the mouse monoclonal antibody in green (B and E) or polymerized actin in red (A and D). Cells were either untreated before staining (A to C) or treated with cytochalasin B (D to F). Panels C and F show the merged actin and iNOS images from panels A and B and panels D and E, respectively; areas of colocalization are shown in yellow. Magnification, ×600 for all panels.

mented in fractions 1 to 3. Enzymatic assay of iNOS from these gradient fractions showed a similar distribution, confirming that this particulate iNOS was enzymatically active (Fig. 4B). Surface biotinylated proteins were identified exclusively in the light region of the gradient (Fig. 4C, lanes 1 and 2), with a distribution similar but not completely identical to that of iNOS. Assay of the lysosomal enzyme β-glucuronidase showed two peaks of activity (Fig. 4D). There was a peak in the denser region of the gradient, consistent with previous reports showing that lysosomes are denser than early components of the endocytic pathway (8, 35). There was, however, another peak in the lighter portion of the gradient, in the same fractions as the surface protein and iNOS. This was a consistent feature of Percoll fractionation of LPS- and IFN-γ-stimulated RAW cells. This lighter density fraction may result from intracellular acidification following macrophage activation, a process that has been reported to lower the density of lysosomes (21). Attempts were made to improve the resolution of the Percoll density gradient separation, but these were not successful. Although the separation is not complete, the data show that particulate iNOS from lysed cells is contained in a light vesicle population that is enzymatically active and distinct from dense lysosomes but is of a density similar to that of vesicles derived from plasma membrane.

Patterns of iNOS localization following phagocytosis. Next, we examined the pattern of iNOS staining within macrophages following phagocytosis of a variety of particles. These included latex beads, zymosan, IgG-coated magnetic beads, and complement-coated zymosan particles. Representative results from experiments with primary macrophages are shown in Fig. 5. Panels A and B show iNOS staining (green) following phagocytosis of latex beads for a 30-min period. iNOS staining remained at the periphery of the cells and did not localize to phagosomes. Similar results were seen at much earlier time points (2 and 5 min of particle internalization; data not shown), with no localization of iNOS to phagosomes at any stage of bead uptake. Following internalization of latex beads, phagosomes were allowed to mature for a further 2 h and the pattern of iNOS distribution was analyzed (Fig. 5D to F). This showed that the majority of latex bead-containing phagosomes had no accumulation of iNOS at their periphery (Fig. 5D). There were occasional phagosomes that showed iNOS accumulation at their periphery (Fig. 5D). However, this was seen in only fewer than 1% of the cells. In contrast, after this period of maturation, most phagosomes showed accumulation of the lysosomal marker LAMP-1 (Fig. 5E and F) confirming the fusion of lysosomes with phagocytosed latex beads at this time after ingestion.

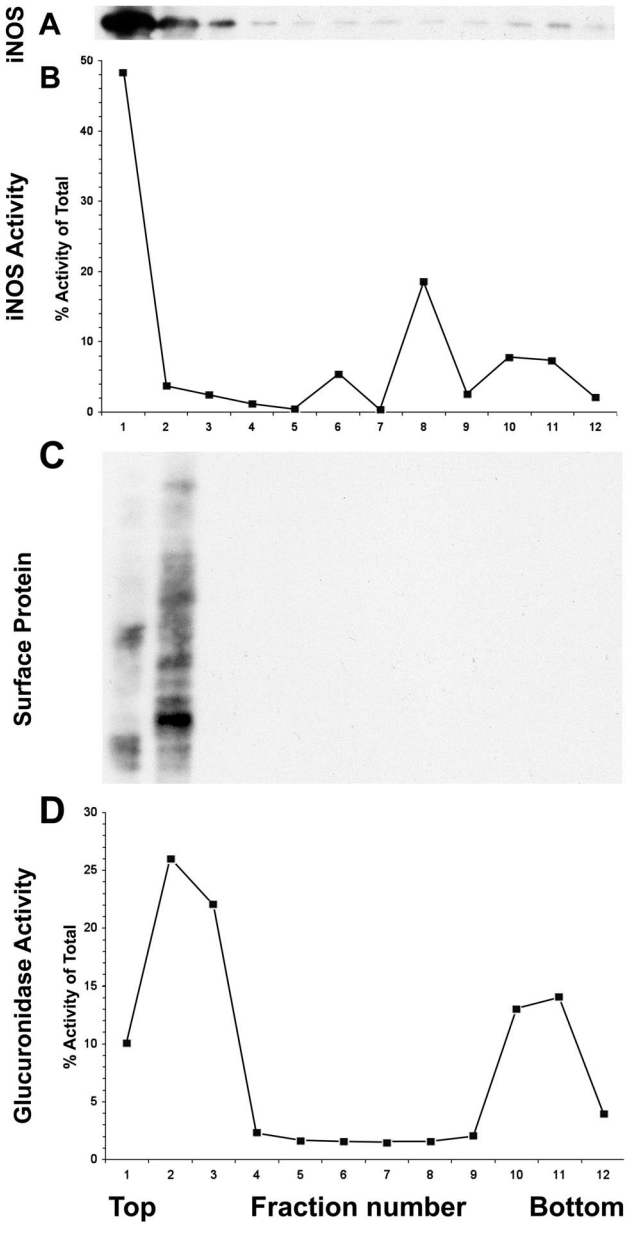

FIG. 4. Density gradient centrifugation analysis of the particulate fraction of IFN-γ- and LPS-treated RAW 264 cells. Each panel shows an assay performed on each of 12 fractions from the density gradient, with the lighter fractions to the left (top) and the denser ones to the right (bottom). The experiment was repeated with similar results. (A) iNOS protein, detected by Western blotting. The band shown is the major band detected, at 135 kDa. So that the bands in lanes 6 to 11 could be seen, the blot was overexposed for lanes 1 to 3. (B) iNOS activity, as assayed by arginine-to-citrulline conversion. (C) Surface proteins of the cell, labeled by surface biotinylation, identified by probing the Western blot with horseradish peroxidase-streptavidin. The gel shows proteins ranging in size from 200 kDa at the top of the panel to 29 kDa at the bottom. (D) β-glucuronidase activity.

Similarly, there was a lack of association of iNOS with phagosomes containing IgG and complement-coated particles at various stages of maturation (Fig. 5G to I and data not shown). When macrophages were allowed to phagocytose zymosan particles, at 2 min after addition cells in which pseudopodial arms were closing around the ingested particle could be observed (Fig. 5C). iNOS appeared to be selectively localized to the point of fusion of the pseudopodial arms under these conditions (Fig. 5C). Fixation of cells exactly at this point of pseudopodial fusion was a relatively rare event, so that the significance of the iNOS staining observed in these cells is difficult to gauge. However, this was observed only with zymosan particles.

iNOS localization following ingestion of *S. enterica* serovar Typhimurium. Using a virulent strain of *S. enterica* serovar Typhimurium labeled with green fluorescent protein, we analyzed the distribution of iNOS following phagocytosis of this microorganism (Fig. 6). In both primary cells (Fig. 6A) and RAW 264 macrophages (Fig. 6B), there was no localization of iNOS around the *Salmonella* vacuole at any stage of maturation (Fig. 6A and B and data not shown). Similar results were obtained using bacteria in either the stationary or logarithmic phase of growth. Serovar Typhimurium prevents the transport of NADPH oxidase to the *Salmonella* vacuole by a process that is dependent on a type III secretory system encoded by a pathogenicity island termed SPI-2 (32). We therefore examined the distribution of iNOS around phagosomes containing an SPI-2 mutant strain (Fig. 6C). At a time when NADPH oxidase had accumulated around phagocytosed bacteria of this strain (38), we did not observe any relocalization of iNOS (Fig. 6C). Furthermore, when we stained macrophages for nitrotyrosine, a marker of the formation of peroxynitrite anions, although this could be seen within cells, it did not localize around phagocytosed bacteria (Fig. 6D).

NO effects on bacterial uptake by macrophages. The presence of iNOS at the plasma membrane is ideal for delivery of NO to potentially pathogenic microorganisms as they undergo phagocytosis. In a previous study of serovar Typhimurium survival within macrophages using IFN-γ-primed macrophages, a delayed bacteriostatic effect of NO production on bacterial proliferation was observed (37). Therefore, a possible explanation of the lack of recruitment of iNOS to the *Salmonella* vacuole observed above is that we had not examined the cells at a point when NO was exerting its antibacterial effect. Therefore, we measured the time course of survival of *Salmonella* within RAW macrophages treated with (i) no additions, (ii) LPS and IFN-γ, (iii) LPS and IFN-γ and the NOS inhibitor L-NIL. Figure 7 shows that at 45 min after infection there was no significant difference in survival of intracellular *Salmonella* among the three groups of cells. However, at 4 h after infection there was a significant reduction in the numbers of intracellular *Salmonella* in the LPS- and IFN-γ-treated cells compared to untreated cells, a difference that was abolished by the NOS inhibitor L-NIL (Fig. 7). Numbers of intracellular bacteria increased by 20 h after infection in all groups, although the difference between the LPS- and IFN-γ-treated group and the others remained. Under these conditions, the NOS inhibitor L-NIL inhibited macrophage NO output by >95%, as detected by a Griess assay (data not shown). Thus, NO does exert an antibacterial effect in these cells, which is evident at 4 h after infection—a time when we observed no recruitment of iNOS to the *Salmonella* vacuole (Fig. 6C and data not shown).

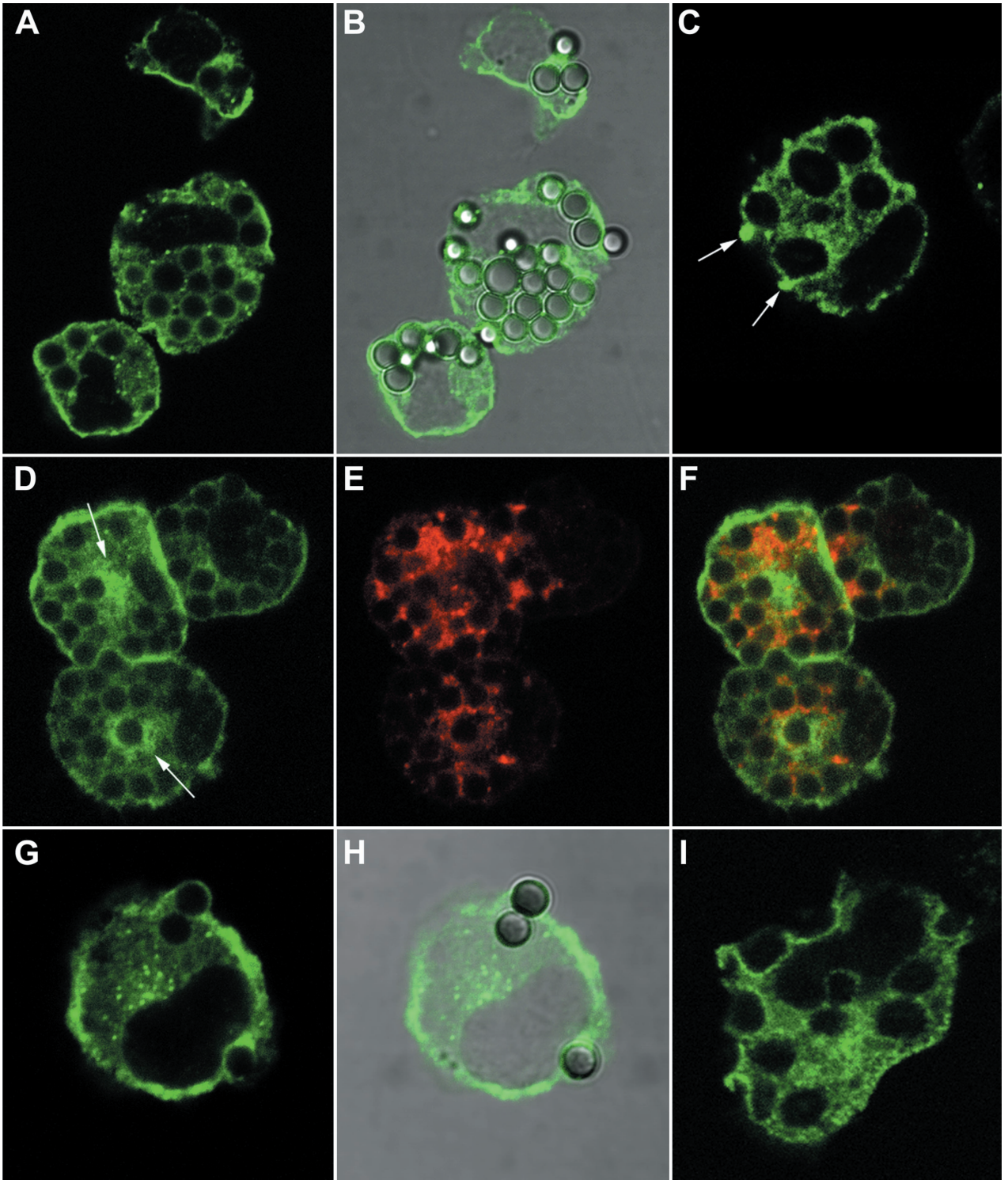

FIG. 5. iNOS distribution following phagocytosis in mouse primary peritoneal macrophages. Cells treated with IFN-γ and LPS were used in all panels. (A and B) Uptake of latex beads at 30 min after addition. iNOS staining (mouse monoclonal) in green is shown alone (A) and also merged with the differential interference contrast (DIC) image of the same cell (B). (C) A cell, 2 min after addition of zymosan particles, stained for iNOS (mouse monoclonal) in green. Accumulation of iNOS at the tips of pseudopodia closing around zymosan just entering the cell is shown by arrows. (D to F) Cells, 2 h after being fed latex beads for 10 min, which were then removed by washing. The panels show the pattern of iNOS staining (mouse monoclonal) in green (D), LAMP-1 staining in red (E), and the merged images of panels D and E (F), where areas of colocalization are shown in yellow. Two areas showing apparent accumulation of iNOS around the outside of phagocytosed beads are indicated by arrows in panel D. (G and H) Uptake of IgG-coated magnetic beads at 5 min after addition. iNOS staining (rabbit polyclonal antibody) in green is shown alone (G) and merged with the DIC image of the same cell (H). (I) A cell, 10 min after the addition of complement-coated zymosan particles stained for iNOS (mouse monoclonal) in green. Magnification, ×2,000 for all panels.

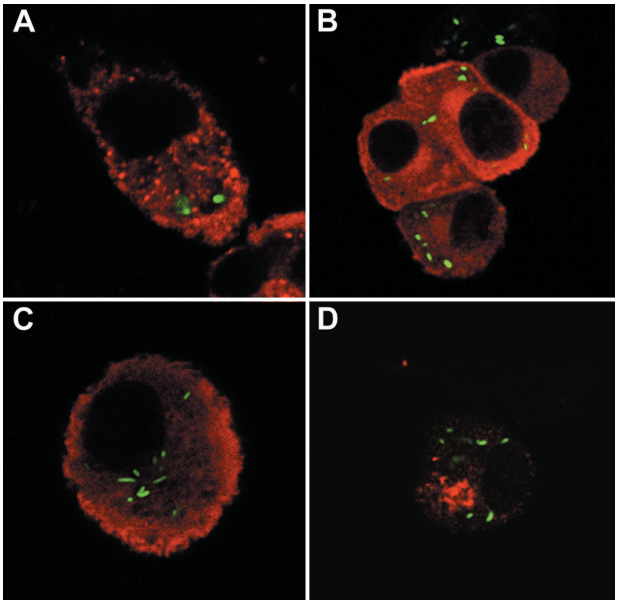

FIG. 6. iNOS and nitrotyrosine in macrophages following phagocytosis of serovar Typhimurium. In all cases, the bacteria are labeled green. (A) iNOS (red; mouse monoclonal) in a primary macrophage 2 h after phagocytosis of wild-type stationary phase serovar Typhimurium. (B) iNOS (red; rabbit polyclonal) in a RAW 264 cell 90 min after phagocytosis of wild-type stationary phase serovar Typhimurium. (C) iNOS (red; rabbit polyclonal) in a RAW 264 cell 4 h after phagocytosis of a SPI-2 mutant stationary-phase serovar Typhimurium. (D) Nitrotyrosine staining (red) in a RAW 264 cell 4 h after phagocytosis of wild-type stationary-phase serovar Typhimurium. Magnification, ×1,000 (B and D) or ×2,000 (A and C).

DISCUSSION

The work presented here reports the novel observation that a proportion of iNOS is associated with the cortical actin cytoskeleton in primary mouse macrophages and the murine macrophage cell line RAW 264. iNOS was also found in an intracellular vesicle population, within the Golgi apparatus, and diffusely within the cytoplasm. Following phagocytosis of a variety of particles, there was little evidence of recruitment of iNOS to phagosomes; neither was there relocation of iNOS around phagocytosed serovar Typhimurium. Although not recruited to the phagosome, cortical iNOS is ideally placed to deliver microbicidal NO to microorganisms in contact with the cell surface.

We also found iNOS diffusely within the cytoplasm, within cytoplasmic vesicles, and in a Golgi compartment (Fig. 1 and 2). The relative distribution of iNOS between these different subcellular sites is difficult to gauge from confocal microscopy, as pixel densities for each component would have to be calculated for multiple confocal sections through each cell to calculate the total distribution of iNOS. From the combined imaging, biochemical fractionation, and activity assays, we estimate that about 20% of iNOS is localized to the cortical region in macrophages following LPS and IFN-γ stimulation under the conditions used here.

What can we deduce about the functional role of the differentially distributed iNOS we have described? We originally hypothesized that iNOS would be targeted to phagosomes, in order to deliver a high concentration of NO to ingested microbes and limit possible damaging effects to the rest of the cell. Cortical iNOS is obviously well placed to deliver NO to incoming microorganisms that are being ingested. However, following phagocytosis of a variety of particles, cortical iNOS is not retained in or recruited to the phagosome (Fig. 5). Similarly, there was no association of iNOS with phagocytosed serovar Typhimurium (Fig. 6). These experiments utilized all the major molecular mechanisms for triggering phagocytosis—the Fc receptor, complement receptors, and the mannose receptor. It seems unlikely, therefore, that failure to observe recruitment of iNOS to the phagosome resulted from lack of signaling from cell surface receptors engaged during phagocytosis. Phagocytosis involves the internalization of a large proportion of the macrophage cell membrane, but only a very small proportion of plasma membrane proteins are removed as a result of this process, the majority being returned to their original locations (22). Integral membrane proteins such as Toll-like receptor 2 and natural resistance-associated macrophage protein 1 (N-RAMP1) are recruited to the phagosomal membrane (16, 36), although in the case of Toll-like receptor 2, this association can be transient. We analyzed iNOS localization around phagosomes at a range of times after formation, including very early stages at 2 min after particle internalization. We do not feel, therefore, that we missed a transient early recruitment of iNOS to the phagosome. The association of iNOS with the cortical actin cytoskeleton, on the cytoplasmic side of the cell membrane (Fig. 3), suggested that it might move with actin to the phagosomal membrane. However, not all actin-associated proteins show such a redistribution. For example, in phagocytosis of unopsonized zymosan, the actin-

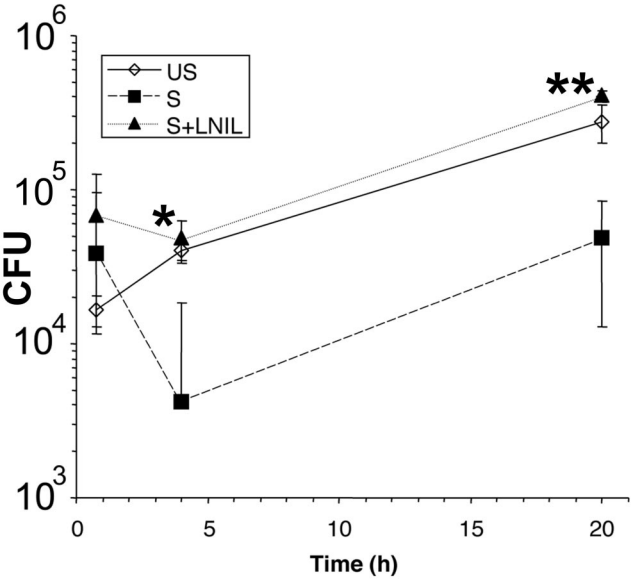

FIG. 7. Survival of serovar Typhimurium within RAW macrophages. Cells were infected at a multiplicity of infection of 10 with 10^7 bacteria at time zero. The graph shows the mean intracellular bacterial numbers found in RAW 264 cells either unstimulated (US), treated with LPS and IFN-γ (S), or treated with LPS and IFN-γ plus L-NIL (S+LNIL). Error bars, ± 1 standard deviation. A significant difference was found in intracellular *Salmonella* survival between cells treated with LPS and IFN-γ and cells treated with LPS, IFN-γ, and L-NIL at 4 and 20 h after infection. *, $P < 0.05$; ** $P < 0.01$ (two-tailed t test).

associated proteins vinculin and paxillin do not associate with phagosomes (1).

Despite the lack of recruitment of iNOS to phagosomes, NO clearly has important antimicrobial actions within macrophages, notably for serovar Typhimurium (37) (Fig. 7). In IFN-γ-treated macrophages (37), this effect, although noticeable at 2 h after bacterial entry, was more marked 10 h after infection. We found that in LPS- and IFN-γ-stimulated cells, the effect was somewhat earlier, with clear NO-dependent killing at 4 h after bacterial entry (Fig. 7). This difference may reflect the time taken for induction of iNOS in IFN-γ-treated macrophages following bacterial ingestion. In LPS- and IFN-γ-stimulated cells, high levels of iNOS are already present, so that the time course of *Salmonella* killing more accurately reflects the time of antimicrobial action of NO against the ingested microbe. However, in vivo, it may be more likely that macrophages are first activated with IFN-γ and then receive an LPS stimulus on phagocytosing *Salmonella*. Thus, the time course of *Salmonella* killing by macrophages in natural infection may be better reflected by cells activated with IFN-γ alone rather than LPS and IFN-γ.

iNOS association with the cortical actin cytoskeleton may be important in targeting NO to bacteria as they enter the cell, although the effects on phagocytosed serovar Typhimurium are not evident until 4 h after uptake of the bacteria into the cell. Alternatively, it may be that NO is capable of antimicrobial action without producing cytotoxicity, even if it is not delivered directly to the *Salmonella* vacuole. Unlike superoxide, NO can readily diffuse across membranes (10) and thus could enter the phagosome from the cytosol. This might account for the localization of the NADPH oxidase but not iNOS to the phagosomal membrane. In addition, the exact identity of the reactive nitrogen species responsible for anti-*Salmonella* activity is unknown. For example, NO may also produce potent antimicrobial compounds by reacting with cytosolic thiols to yield *S*-nitrosothiols. These reactions may be facilitated by cytosolic localization of NO production by iNOS. To determine the contribution of cortical actin-associated iNOS to *Salmonella* killing will require the construction of iNOS mutants that are specifically targeted to either plasma membrane or cytoplasm. Cells expressing these differently localized enzymes can then be assayed for their ability to affect intracellular *Salmonella* replication.

Serovar Typhimurium has evolved mechanisms which enable it to avoid contact with the NADPH oxidase within macrophages, as revealed by SPI-2 mutants (38). These mutants, however, also failed to show accumulation of iNOS around phagocytosed bacteria (Fig. 6C). Although *Salmonella* may have other genes which encode a factor able to prevent iNOS localization around phagosomes, we feel that this is very unlikely, since a variety of experimental particles also failed to show iNOS recruitment to the phagosome (Fig. 5). In addition, we did not observe any iNOS accumulation around phagocytosed *E. coli*, which enters but does not proliferate within macrophages (data not shown). It has been assumed that peroxynitrite, the product of NO and superoxide, is a major antimicrobial factor within macrophages (41). However, Vazquez Torres et al. (37) showed no localization of nitrotyrosine around intracellular *Salmonella* and found that the peroxynitrite scavenger uric acid potentiates rather than inhibits *Salmonella* killing. In addition, there was a clear temporal separation of the roles of NADPH oxidase and iNOS in *Salmonella* killing. Thus, it seems unlikely that peroxynitrite is responsible for macrophage killing of intracellular *Salmonella*. Although there was evidence of nitrotyrosine generation within macrophages in our experiments, we too found no localization around phagocytosed bacteria (Fig. 6D), unlike the extensive nitration around phagocytosed *Staphylococcus aureus* within neutrophils (13). It may be that bacterial peroxiredoxins in *Salmonella* are able to detoxify peroxynitrite within the vicinity of the bacterium, avoiding nitration (6). However, deletion of the gene for the small subunit of the peroxiredoxin alkylhydroperoxide reductase in serovar Typhimurium does not affect virulence, suggesting that such a mechanism is not critical for pathogenesis. An alternative explanation for the absence of nitration of intracellular *Salmonella* might be the abundance of periplasmic superoxide dismutase in the bacteria, limiting in situ formation of peroxynitrite from NO and superoxide (9, 14, 15).

One previous report analyzed the subcellular distribution of iNOS in primary macrophages using immunoelectron microscopy (39). These authors found that iNOS was both cytoplasmic and in a vesicle population, particularly at the *trans* face of the Golgi apparatus, and with some staining at the cell periphery. A notable feature of the cells showing the most marked membrane iNOS staining in the present study is that they had a rounded, nonactivated shape, even after LPS and IFN-γ stimulation. Thioglycolate-induced macrophages can show a more activated macrophage phenotype, with extension of multiple pseudopodia (12). Cells with this morphology tended not to show plasma membrane iNOS, suggesting that the signal involved in the generation of this phenotype leads to loss of iNOS from this site. Differences in macrophage activation state may thus account for differences in iNOS distribution.

Cortical iNOS might be involved not in microbial killing but in some other function. Recently, an essential role for NO derived from iNOS has been demonstrated in the signaling pathway of interleukin 12 (IL-12) and IFN-α/β within NK cells (11). Plasma membrane-associated iNOS would be well placed to deliver NO locally to the IL-12 receptor signaling complex, maximizing its signaling effects while limiting toxicity within the cell. Macrophages have recently been shown to respond to combined IL-12 and IL-18 stimulation with an increased output of IFN-γ (24). Whether NO participates in the IL-12 signaling pathway in macrophages remains to be determined.

What mechanism underlies the association of iNOS with the cortical actin cytoskeleton? It has been found that in epithelial cells, iNOS is localized to the apical membrane of polarized cells (P. Glynne and T. J. Evans, submitted for publication). The interaction of iNOS with membranes from these epithelial cells shows that iNOS is a tightly bound peripheral protein, associating with the cortical actin cytoskeleton and requiring mixtures of salt and detergent for efficient solubilization. This suggests that similar molecular mechanisms are involved in tethering iNOS to the cortical region in all these cells. iNOS does not have an intrinsic membrane-spanning domain, nor does it have known lipid modifications, suggesting that the most likely mechanism is by a direct protein-protein interaction with a component of the cortical actin cytoskeleton. The Golgi association may thus reflect the trafficking of iNOS in

association with this protein through the cell on its way to the cell cortex.

iNOS is an important part of the phagocyte's defensive capabilities, and the work described here sheds more light on the way in which it is controlled by the cell. Further work with additional pathogens will better define the precise role that membrane-associated iNOS has in microbial killing and may reveal additional functions of iNOS.

ACKNOWLEDGMENTS

We thank Julia Polak for providing facilities for confocal microscopy.

This work was supported by the Wellcome Trust and the Lister Institute by the award of a Jenner Fellowship to T.J.E.

REFERENCES

1. **Allen, L. A., and A. Aderem.** 1996. Molecular definition of distinct cytoskeletal structures involved in complement- and Fc receptor-mediated phagocytosis in macrophages. J. Exp. Med. **184:**627–637.
2. **Beckman, J. S., and J. N. Siedow.** 1985. Bactericidal agents generated by the peroxidase-catalyzed oxidation of para-hydroquinones. J. Biol. Chem. **260:** 14604–14609.
3. **Beuzon, C. R., S. Meresse, K. E. Unsworth, J. Ruiz-Albert, S. Garvis, S. R. Waterman, T. A. Ryder, E. Boucrot, and D. W. Holden.** 2000. Salmonella maintains the integrity of its intracellular vacuole through the action of SifA. EMBO J. **19:**3235–3249.
4. **Borregaard, N., J. M. Heiple, E. R. Simons, and R. A. Clark.** 1983. Subcellular localization of the b-cytochrome component of the human neutrophil microbicidal oxidase: translocation during activation. J. Cell Biol. **97:**52–61.
5. **Brune, B., A. von Knethen, and K. B. Sandau.** 1998. Nitric oxide and its role in apoptosis. Eur. J. Pharmacol. **351:**261–272.
6. **Bryk, R., P. Griffin, and C. Nathan.** 2000. Peroxynitrite reductase activity of bacterial peroxiredoxins. Nature **407:**211–215.
7. **Buchmeier, N. A., and F. Heffron.** 1991. Inhibition of macrophage phagosome-lysosome fusion by *Salmonella typhimurium*. Infect. Immun. **59:**2232–2238.
8. **Claus, V., A. Jahraus, T. Tjelle, T. Berg, H. Kirschke, H. Faulstich, and G. Griffiths.** 1998. Lysosomal enzyme trafficking between phagosomes, endosomes, and lysosomes in J774 macrophages. Enrichment of cathepsin H in early endosomes. J. Biol. Chem. **273:**9842–9851.
9. **De Groote, M. A., U. A. Ochsner, M. U. Shiloh, C. Nathan, J. M. McCord, M. C. Dinauer, S. J. Libby, A. Vazquez-Torres, Y. Xu, and F. C. Fang.** 1997. Periplasmic superoxide dismutase protects Salmonella from products of phagocyte NADPH-oxidase and nitric oxide synthase. Proc. Natl. Acad. Sci. USA **94:**13997–14001.
10. **Denicola, A., J. M. Souza, R. Radi, and E. Lissi.** 1996. Nitric oxide diffusion in membranes determined by fluorescence quenching. Arch. Biochem. Biophys. **328:**208–212.
11. **Diefenbach, A., H. Schindler, M. Rollinghoff, W. M. Yokoyama, and C. Bogdan.** 1999. Requirement for type 2 NO synthase for IL-12 signaling in innate immunity. Science **284:**951–955.
12. **Doyle, A. G., and I. P. Fraser.** 1998. Murine macrophages: isolation, cultivation, and characterization, p. 154.1–154.8. *In* D. M. Weir (ed.), Experimental immunology, 5th ed. Blackwell Scientific, Oxford, United Kingdom.
13. **Evans, T. J., L. D. K. Buttery, A. Carpenter, D. R. Springall, J. M. Polak, and J. Cohen.** 1996. Cytokine-treated human neutrophils contain inducible nitric oxide synthase that produces nitration of ingested bacteria. Proc. Natl. Acad. Sci. USA **93:**9553–9558.
14. **Fang, F. C., M. A. DeGroote, J. W. Foster, A. J. Baumler, U. Ochsner, T. Testerman, S. Bearson, J. C. Giard, Y. Xu, G. Campbell, and T. Laessig.** 1999. Virulent Salmonella typhimurium has two periplasmic Cu, Zn-superoxide dismutases. Proc. Natl. Acad. Sci. USA **96:**7502–7507.
15. **Figueroa-Bossi, N., and L. Bossi.** 1999. Inducible prophages contribute to Salmonella virulence in mice. Mol. Microbiol. **33:**167–176.
16. **Gruenheid, S., E. Pinner, M. Desjardins, and P. Gros.** 1997. Natural resistance to infection with intracellular pathogens: the Nramp1 protein is recruited to the membrane of the phagosome. J. Exp. Med. **185:**717–730.
17. **Hiki, K., Y. Yui, R. Hattori, H. Eizawa, K. Kosuga, and C. Kawai.** 1991. Cytosolic and membrane-bound nitric oxide synthase. Jpn. J. Pharmacol. **56:**217–220.
18. **Ischiropoulos, H., L. Zhu, J. Chen, M. Tsai, J. C. Martin, C. D. Smith, and J. S. Beckman.** 1992. Peroxynitrite-mediated tyrosine nitration catalysed by superoxide dismutase. Arch. Biochem. Biophys. **298:**431–437.
19. **Kroncke, K. D., K. Fehsel, and V. Kolb-Bachofen.** 1997. Nitric oxide: cytotoxicity versus cytoprotection—how, why, when, and where? Nitric Oxide **1:**107–120.
20. **MacMicking, J., Q. W. Xie, and C. Nathan.** 1997. Nitric oxide and macrophage function. Annu. Rev. Immunol. **15:**323–350.
21. **Mayorga, L. S., M. G. De Veca, M. I. Colombo, and F. Bertini.** 1993. Effect of pH and ATP on the equilibrium density of lysosomes. J. Cell. Physiol. **156:**303–310.
22. **Mellman, I.** 2000. Quo vadis: polarized membrane recycling in motility and phagocytosis. J. Cell Biol. **149:**529–530.
23. **Mullock, B. M., N. A. Bright, C. W. Fearon, S. R. Gray, and J. P. Luzio.** 1998. Fusion of lysosomes with late endosomes produces a hybrid organelle of intermediate density and is NSF dependent. J. Cell Biol. **140:**591–601.
24. **Munder, M., M. Mallo, K. Eichmann, and M. Modolell.** 1998. Murine macrophages secrete interferon gamma upon combined stimulation with interleukin (IL)-12 and IL-18: a novel pathway of autocrine macrophage activation. J. Exp. Med. **187:**2103–2108.
25. **Murad, F.** 1998. Nitric oxide signaling: would you believe that a simple free radical could be a second messenger, autacoid, paracrine substance, neurotransmitter, and hormone? Recent Prog. Horm. Res. **53:**43–60.
26. **Nathan, C.** 1997. Inducible nitric oxide synthase: what difference does it make? J. Clin. Investig. **100:**2417–2423.
27. **Nathan, C., and Q.-W. Xie.** 1994. Regulation of biosynthesis of nitric oxide. J. Biol. Chem. **269:**13725–13728.
28. **Palacios, M., J. Padron, L. Glaria, A. Rojas, R. Delgado, R. Knowles, and S. Moncada.** 1993. Chlorpromazine inhibits both the constitutive nitric oxide synthase and the induction of nitric oxide synthase after LPS challenge. Biochem. Biophys. Res. Commun. **196:**280–286.
29. **Radi, R., J. S. Beckman, K. M. Bush, and B. A. Freeman.** 1991. Peroxynitrite-induced membrane lipid peroxidation: the cytotoxic potential of superoxide and nitric oxide. Arch. Biochem. Biophys. **288:**481–487.
30. **Schmidt, H. H., T. D. Warner, M. Nakane, U. Forstermann, and F. Murad.** 1992. Regulation and subcellular location of nitrogen oxide synthases in RAW264.7 macrophages. Mol. Pharmacol. **41:**615–624.
31. **Schoedon, G., M. Schneemann, S. Hofer, L. Guerrero, N. Blau, and A. Schaffner.** 1993. Regulation of the L-arginine-dependent and tetrahydrobiopterin-dependent biosynthesis of nitric oxide in murine macrophages. Eur. J. Biochem. **213:**833–839.
32. **Shiloh, M. U., and C. F. Nathan.** 2000. Reactive nitrogen intermediates and the pathogenesis of Salmonella and mycobacteria. Curr. Opin. Microbiol. **3:**35–42.
33. **Stuehr, D. J.** 1999. Mammalian nitric oxide synthases. Biochim. Biophys. Acta **1411:**217–230.
34. **Tian, Y., Y. Xing, R. Magliozzo, K. Yu, B. R. Bloom, and J. Chan.** 2000. A commercial preparation of catalase inhibits nitric oxide production by activated murine macrophages: role of arginase. Infect. Immun. **68:**3015–3018.
35. **Tjelle, T. E., A. Brech, L. K. Juvet, G. Griffiths, and T. Berg.** 1996. Isolation and characterization of early endosomes, late endosomes and terminal lysosomes: their role in protein degradation. J. Cell Sci. **109:**2905–2914.
36. **Underhill, D. M., A. Ozinsky, A. M. Hajjar, A. Stevens, C. B. Wilson, M. Bassetti, and A. Aderem.** 1999. The Toll-like receptor 2 is recruited to macrophage phagosomes and discriminates between pathogens. Nature **401:** 811–815.
37. **Vazquez Torres, A., J. Jones Carson, P. Mastroeni, H. Ischiropoulos, and F. C. Fang.** 2000. Antimicrobial actions of the NADPH phagocyte oxidase and inducible nitric oxide synthase in experimental salmonellosis. I. Effects on microbial killing by activated peritoneal macrophages in vitro. J. Exp. Med. **192:**227–236.
38. **Vazquez Torres, A., Y. Xu, J. Jones Carson, D. W. Holden, S. M. Lucia, M. C. Dinauer, P. Mastroeni, and F. C. Fang.** 2000. Salmonella pathogenicity island 2-dependent evasion of the phagocyte NADPH oxidase. Science **287:** 1655–1658.
39. **Vodovotz, Y., C. Bogdan, J. Paik, Q.-W. Xie, and C. Nathan.** 1993. Mechanisms of suppression of macrophage nitric oxide release by transforming growth factor b. J. Exp. Med. **178:**605–613.
40. **Xie, Q.-W., H. J. Cho, J. Calaycay, R. A. Mumford, K. M. Swiderek, T. D. Lee, A. Ding, T. Troso, and C. Nathan.** 1992. Cloning and characterization of inducible nitric oxide synthase from mouse macrophages. Science **256:**225–228.
41. **Zhu, L., C. Gunn, and J. Beckman.** 1992. Bactericidal activity of peroxynitrite. Arch. Biochem. Biophys. **298:**452–457.

Editor: V. J. DiRita